Published in final edited form as:
Cell Mol Bioeng. 2012 June ; 5(2): . doi:10.1007/s12195-012-0226-y.

Low Concentration Microenvironments Enhance the Migration of Neonatal Cells of Glial Lineage

Richard A. Able Jr.[1,2], **Celestin Ngnabeuye**[1], **Cade Beck**[1], **Eric C. Holland**[3], and **Maribel Vazquez**[1]

[1]Department of Biomedical Engineering, The City College of The City University of New York (CCNY), 160 Convent Avenue, Steinman Hall Room 403D, New York, NY 10031, USA

[2]Department of Biochemistry, The City Graduate Center of The City University of New York (CCNY), 365 Fifth Avenue, New York, NY 10016, USA

[3]Department of Neurosurgery, Memorial Sloan Kettering Cancer Center, New York, NY 10021, USA

Abstract

Glial tumors have demonstrated abilities to sustain growth *via* recruitment of glial progenitor cells (GPCs), which is believed to be driven by chemotactic cues. Previous studies have illustrated that mouse GPCs of different genetic backgrounds are able to replicate the dispersion pattern seen in the human disease. How GPCs with genetic backgrounds transformed by tumor paracrine signaling respond to extracellular cues *via* migration is largely unexplored, and remains a limiting factor in utilizing GPCs as therapeutic targets. In this study, we utilized a microfluidic device to examine the chemotaxis of three genetically-altered mouse GPC populations towards tumor conditioned media, as well as towards three growth factors known to initiate the chemotaxis of cells excised from glial tumors: Hepatocyte Growth Factor (HGF), Platelet-Derived Growth Factor-BB (PDGF-BB), and Transforming Growth Factor-α (TGF-α). Our results illustrate that GPC types studied exhibited chemoattraction and chemorepulsion by different concentrations of the same ligand, as well as enhanced migration in the presence of ultra-low ligand concentrations within environments of high concentration gradient. These findings contribute towards our understanding of the causative and supportive roles that GPCs play in tumor growth and reoccurrence, and also point to GPCs as potential therapeutic targets for glioma treatment.

Keywords

Chemotaxis; TGF-α; Microfluidics; Glial progenitors; Glioma; Concentration gradients; RCAS tv-a

INTRODUCTION

Gliomas are the most common form of primary brain cancer present in adults, affecting 10% of the worldwide cancer population and harboring a 5-year survival rate of less than 25%.[8,67,76] These glial tumors pose unique clinical challenges because their aggressive migration within healthy brain tissue minimizes the effectiveness of surgical resection.[1,51,68] A wealth of evidence now demonstrates that bulk tumor growth can occur *via* extensive cell

Address correspondence to Maribel Vazquez, Department of Biomedical Engineering, The City College of The City University of New York (CCNY), 160 Convent Avenue, Steinman Hall Room 403D, New York, NY 10031, USA. vazquez@ccny.cuny.edu.

proliferation,[12,53,62] as well as by aggressive recruitment of surrounding cells.[3,9,21,72] Glial tumors have demonstrated the ability to recruit a variety of cells *via* paracrine signaling to maintain and extend tumor survival,[22] including stem cells,[28,49] endothelial cells,[25] macrophages[79] and endogenous precursors,[3,29] or glial progenitor cells (GPCs).

A recent *in vivo* study demonstrated that GPCs were able to migrate from the brain subventricular zone (SVZ) towards pre-existing glial tumors and then surround the tumor mass.[17,22] Such GPC recruitment by glial tumors is believed to be driven by chemotactic cues, i.e. chemical concentration gradients that stimulate cell migration towards a tumor mass.[67,88] Studies using mouse glial progenitors have demonstrated that different populations of GPCs exhibit distinct patterns of migration that are replicated in the human disease. [6,64] For example, populations of GPCs have been seen to invade the brain as individual cells, as well as *via* chain cell migration along the vasculature.[58,65] Interestingly, such differences in migratory phenotype have been seen across cells where the intracellular signaling was accomplished *via* the same pathway.[58,65] Whether distinct GPC migratory phenotypes become acquired with genetic backgrounds altered *via* tumor paracrine signaling is unknown. Further, how genetically transformed cells respond to extracellular cues *via* migration is largely unexplored, and remains a limiting factor in utilizing GPCs as therapeutic targets.

In this study we examine the *in vitro* migration of varying populations of genetically-altered GPCs in order to examine how defined microenvironments affect the chemotaxis of the different GPC populations. We examine the growth factor-induced migration of cells derived from three primary mouse GPC types and one primary mouse tumor alongside two well-studied human glioblastoma cell lines. Here, we examine the chemoattractant strength of three principle growth factors Hepatocyte Growth Factor (HGF), Platelet-Derived Growth Factor Beta (PDGF-B), and Transforming Growth Factor Alpha (TGF-α) because of the extensive evidence that documents their induced migration of cells derived from glial tumors.[7,18,19,40,55,59] Our results illustrate that despite the different migratory mechanisms employed by the GPC types, all GPCs exhibited chemoattraction and chemorepulsion by different concentrations of the same ligand, as well as enhanced migration in the presence of ultra-low ligand concentrations within environments of high concentration gradient. In addition, all GPCs studied were observed to migrate much shorter distances than their glioblastoma-derived counterparts, suggesting that glial tumors may recruit and/or transform highly localized GPCs to enhance growth. Our study provides data to merit examination of GPCs as potential drug delivery vehicles to the bulk tumor mass, and adds to the growing body of literature that points towards the study of GPC migration as a means to reduce tumor recurrence and/or growth. Lastly, our study is the first to document glial chemoresponsiveness within low concentration environments, which has been previously unexplored in the literature and can significantly impact the testing of therapeutic agents tailored to glioma therapy.

MATERIALS AND METHODS

Cell Culture

Three glial progenitor mouse cell types, one primary mouse tumor and two human tumor cell lines were used in this study. The GPCs of varying genetic backgrounds were chosen because they each represent a cell population that is associated with specific types of tumors present within human brain. GPCs were derived from the RCAS/Ntv-a system from the laboratory of Dr. Eric C. Holland laboratory at Memorial Sloan Kettering Cancer Center, New York.[26,31,52] The Ntv-a transgenic mouse line is comprised of retroviral vectors and mice transgenic for cell type specific expression of the retroviral receptor, tv-a. Briefly, the Ntv-a transgenic mouse line was constructed by expressing tv-a as a transgene from the

nestin promoter. The RCAS viral vectors are avian-specific and only infect mammalian cells engineered to express the tv-a receptor. The Ntv-a system accomplishes glial-specific gene transfer, which permits study of the role of single and multiple mutations in transformed cells of glial lineage.

The four mouse cell types derived from the Ntv-a system used in this study were: (a) GPC^{LacZ} cells: GPCs infected with the RCAS vector to express β-galactosidase[41] and used as our control cell type. These cells do not harbor genetic abnormalities specifically associated with glial tumors, but rather represent a progenitor cell type found in different regions of the brain that can be recruited to aid in tumor growth[12] (b) GPC^{PDGF} cells: GPCs infected with the RCAS vector to develop an autocrine Platelet-Derived Growth Factor (PDGF)-Platelet-Derived Growth Factor Receptor (PDGFR) loop.[12] These cells have been engineered to mimic the characteristics of cells present in astrocytomas, where a PDGF autocrine loop is believed to be responsible for increased proliferation as well as enhanced group migration in the brain[12,45] (c) GPC^{kRas} cells: GPCs infected with RCAS vector that generates constitutively-activated downstream Ras pathways.[32] These cells are characteristic of oligodendrocytomas that present with large diffuse spreading of cells which maintain contact with one another in the brain[33,63] and (d) XFM^{PDGF} cells: Derived from a mouse oligodendrocytoma engineered to express secreted PDGF-B in mice with a INK4a-$Arf^{-/-}$ background.[26,69] The XFM^{PDGF} and GPC^{PDGF} cells are similar in their ability to produce and respond to their own PDGF, but XFM^{PDGF} cells have the INK4a-Arf locus deleted, disabling possible tumor suppressor capabilities. Note that GPC^{LacZ}, GPC^{PDGF} and GPC^{kRas} cells were generated *via* RCAS infection in culture dishes, while XFM^{PDGF} cells were harvested from an excised, induced mouse tumor as shown in Fig. 1. In addition, the two human glioblastoma cell lines studied were U-87 MG (ATCC Cat # HTB-14™) and U-251 MG (ATCC Cat # HTB-17™). These cell lines were examined alongside GPCs because they have been extensively used in glioma research, both *in vivo* and *in vitro*.

All cells were cultured using sterile Dulbecco's Modified Eagle Medium (DMEM) (Cat#: 10-017-CV, Mediatech, VA), supplemented with 2% L-Glutamine (Cat#: 25-015-CI, Mediatech, VA), 2% Penicillin-Streptomycin–Amphotericin B—100× solution (Cat#: 30-002-CI, Mediatech, VA), and 10% fetal bovine serum (FBS) (Cat#: MT35-010-CV, Mediatech, VA). The cells were grown onto sterile polystyrene tissue culture flasks (BD Biosciences, Franklin Lakes, NJ) and incubated at 37 °C with 5% CO_2.

Growth Factors

Three growth factors were used to examine chemotaxis in this study: Hepatocyte Growth Factor/Scatter Factor (HGF) (Molecular Weight = 80 kDa) (Cat#: 2207-HG/SF, R&D Systems, MN), Platelet Derived Growth Factor-BB (PDGF) (Molecular Weight = 12.4 kDa) (Cat#: 220-BB, R&D Systems, MN), and Transforming Growth Factor α (TGF-α) (Molecular Weight = 6 kDa) (Cat#: 616430, Calbiochem & Oncogene, CA). Growth factors were diluted with serum-free DMEM to obtain a concentration range for each experiment between 1 pM and 10 nM.

Chemotaxis Assays

Cellular chemotaxis in response to extracellular signaling from growth factors was analyzed *via* transwell assays, as described previously.[7,50] Briefly, a modified thick coating volume of 200 μL of 0.5 mg/mL Matrigel™ (Cat#: 356230, BD Bioscience, MA) was used to coat the polyethylene terephthalate (PET) membranes with 8 μm-diameter pores, which separated the upper and lower chambers of the transwell system. The matrix was polymerized after a 3-h incubation period at 37 °C, and the uncovered culture plates were placed into a class II biological flow hood for 48 h to dry. Upon drying, plates were wrapped in aluminum foil

and stored at 4 °C for future experiments. Coated filters were rehydrated with 200 μL serum free DMEM and incubated at 37 °C for 1-h immediately prior to their use.

Growth factor solutions between 1 pM and 10 nM concentrations were added to the lower chamber of a 24-well plate (Cat#: BD353047, BD Bioscience, MA), while cell solutions at a density of 1.5×10^6 cells per mL of supplemented DMEM were added to the upper chamber culture inserts (Cat#: BD353097, BD Bioscience, MA). The transwell assay was incubated for 12 h at 37 °C to allow cells migrate through the porous membrane, after which excess cell solution was aspirated from culture inserts. Cells on the upper side of the membrane were removed, and cells on the lower side of the membrane were fixed and stained with Diff-Quick® Stain Set (Dade Behring, DE) to facilitate cell counting. The nuclei of cells that migrated to the underside of the membrane were counted using an inverted light microscope with a 20× objective (Nikon TE300, Morrell Instruments, NY). Cells located within five areas of the culture inserts were counted upon each filter using a checkerboard pattern[87] for a total of five rectangular locations of 0.58 mm × 0.44 mm. These data were used to gather representative cell counts per experiment ($n > 7$).

Conditioned Media Chemotaxis Assays

Cells derived from U-87, U-251, and XFM^{PDGF} tumors were grown separately in T-75 tissue culture flasks in supplemented DMEM. Once 90–95% confluence was reached, complete media was replaced with 10 mL of serum-free DMEM and cells were incubated for 24–48 h. Supernatant was collected and serially diluted in serum-free DMEM to concentration ratios of 1:0 (100% or non-diluted), 1:1 (50%), and 1:4 (25%). Conditioned media (CM) was used in lieu of growth factor solutions within transwell assays for these sets of experiments ($n \geq 3$). Conditioned media of tumor cell samples (U-87, U-251, and XFM^{PDGF}) was collected by serum starving respective cells for 24–48 h prior to testing. In this way, we better examined the migration of GPCs to growth factors generated by the tumor cell samples themselves, without the influence of serum, as done previously in the literature.[5,23,66,71]

Relative Chemoattractant Factor (RCF)

Cell migration indexes are reported here using a parameter called the Relative Chemoattractant Factor (RCF). RCF is defined as the normalized cell count per experiment, and is determined by dividing the average number of cells that migrated towards the test solutions, N_{Test}, by the average number of cells that migrated towards the control solution (in this case serum-free DMEM), N_{Control}. In this way, RCF represents the fold increase in cell migration from control experiments to experimental conditions, as described by Eq. (1).

$$\text{RCF} = \frac{N_{\text{Test}}}{N_{\text{Control}}} \quad (1)$$

Statistical Analysis

RCF values calculated during migration assays were analyzed by analysis of variance (ANOVA) to determine the statistical differences between experimental groups and Student's t test to determine the statistical differences between individual experimental groups and controls. p values less than 0.05 were defined as statistically significant (*).

Antibodies and Immunocytochemistry

Sequential, double immunofluorescence for detection of growth factor receptors was performed as described previously.[14] Briefly, cells grown on coverslips were fixed for 15

min at room temperature with paraformaldehyde (Cat#: P6148, Sigma, St. Louis, MO) and labeled with rabbit polyclonal anti-β-actin (1:1000) (Cat#: ab8227, Abcam, Cambridge, MA), rabbit monoclonal anti-phosphorylated-EGF-R (1:500) (Cat#: ab40815, Abcam, Cambridge, MA), anti-rabbit AlexaFluor® 488 or 594 antibodies (Cat#: A11034 and A11037, respectively, Invitrogen, Camarillo, CA).

Immunoblotting and Detection

Protein lysates were generated from 90 to 95% confluent serum starved cells grown in 100-mm culture plates and done in triplicate (Becton-Dickinson, MA). All cells were serum starved for 2 h in 1× PBS at 37 °C and separately stimulated for 20 min using the specified growth factor concentrations that correlated with maximum RCF values determined from transwell assays. Cells were lysed at 4 °C on ice in cold lysis buffer (Cat#: 2978-50, Sigma, MO) containing 70 μL Protease Inhibitor (Cat#: 78425, Pierce IL), 2 mM phenylmethylsulfonyl fluoride (Cat#: P7626, Sigma-Aldrich MO) and 10 μL Phosphatase Inhibitor Cocktail 2 (Cat#: P5726, Sigma-Aldrich MO) for 15 min. Proteins, 40 μg/well, were separated by 8–16% Tris-Glycine SDS-PAGE precast gels (CAT#58519, Lonza, Rockland, ME), then transferred to nitrocellulose membranes. The stimulation of EGFR tyrosine phosphorylation in GPC^{LacZ} by 1 pM TGF-α, in GPC^{PDGF} by 100 pM TGF-α, and in GPC^{kRas} by 1 pM TGF-α (Fig. 6) was accomplished *via* a 20 min incubation period in the presence of the designated growth factor concentration.

Detection of protein expression was performed using corresponding primary antibodies, the IRDye® 800 CW goat polyclonal anti-rabbit secondary (Cat#: 926-32211, LiCor Biosciences, Lincoln, NE) and the Odyssey Infrared Scanner at 795 nm (LiCor Biosciences, Lincoln, NE). An average intensity measurement, I, was made by selecting a rectangular region (created *via* the Odyssey software's select tool) that encompassed the entire band area of a membrane to record its intensity during imaging. The identical rectangular region was then overlaid onto remaining band areas to determine the average intensity for each band. The average intensity of each experimental condition (e.g. growth factor-stimulated or not) was then divided by the average intensity of the control condition. In this manner, the intensity of control bands have been normalized to $I = 1$, such that reported values of average intensity for experimental conditions reflect a fold-increase or fold-decrease compared to controls.

Confocal Microscopy

Confocal laser scanning microscopy imaging was performed using a Leica TCS SP2 instrument with a HCX PL APO CS 63× oil immersion objective (NA 1.4). Imaging conditions used for each set of experiments were set with Ar/HeNe Laser at 20%; a 1024 × 1024 format; gain range of 600–700 V; 0.5% offset; and a 200-Hz scanning speed.

μLane System

The laboratory-developed μLane system used for this study has been previously described.[38,39] In brief, systems are comprised of a 5-cm-long glass microscope slide bonded to a polydimethylsiloxane (PDMS) elastomer. As shown in Figs. 2a and 2b, the design includes a sink reservoir ($V = 200$ μL), and a source reservoir ($V = 10$ μL). The reservoirs are connected by a single microchannel of 100 μm by 100 μm crosssection and 1.5 cm length. The system works *via* diffusion, whereby growth factors present in high concentration in the source reservoir and channel diffuse towards lower concentration within the sink reservoir to create concentration gradients that stimulate cell migration. In these tests, the microchannel was first filled with a solution of 2 μg/mL of growth factor reduced Matrigel™ (BD Bioscience, MA, Cat: 354230) containing a desired growth factor concentration and incubated at 37 °C for 1.5 h to enable Matrigel™ polymerization. All

experiments were performed using growth factor reduced Matrigel™ as the control ECM. Then, excess matrix was aspirated from the sink reservoir and replaced with cell solution at a density of 1.5×10^6 cells/mL. The system was then incubated at 37 °C. Cell movement into the microchannel from the sink reservoir was monitored *via* light microscopy using a 20× long working distance dry objective and a cooled CCD camera. Images of cells moving from the sink reservoir into the microchannel were recorded at $t = 12$ h, $t = 24$ h, and $t = 36$ h using Nikon software (Nikon Instrument Element 2.30 with 6D module, Morrell Instrument Company Inc., Melville, NY). The numbers of cells that migrated into the microchannels were counted within three regions within the channel, 0–200 μm, 200–400 μm, and 400–600 μm. Experiments were completed in triplicate using newly fabricated μLane systems for each experiment.

Mathematical Modeling

Diffusion within the μLane system was modeled using Fick's Law described by Eq. (2).

$$\frac{\partial C}{\partial t} = D\frac{\partial C}{\partial x} \quad (2)$$

where C is concentration (ng/mL), t (s) is time, D (m^2/s) is the diffusion coefficient, and x (m) is distance. 1-D modeling was appropriate for this system because the channel length, L, was substantially larger than its diameter, D, with $L/D > 100$. Equation (2) was solved using Finite-element-analysis software Matlab 7.7 (Math Works, Natick, MA), with an initial concentration, C_0, set throughout the channel length that was either 10 pM or 100 pM, as per experiment. The boundary conditions were fixed at $C = 0$ at $x = 0$, i.e. entrance of the channel from the sink reservoir, and $C = C_0$ at $x = L$, i.e. the entrance of the channel at the source reservoir end, for all time, t. Analysis *via* Fick's law enabled computation of concentration profiles within the μLane for all times. The simulation revealed that the concentration distribution within the microchannel reached steady-state at $t = 103$ h, after which no changes in concentration with time were seen. Concentration gradients were obtained by calculating the change in concentration along the channel length as done previously[15] *via* Eq. (3):

$$G = \frac{\partial C}{\partial x} \quad (3)$$

where G is gradient, C is concentration (ng/mL), and x (m) is distance.

RESULTS

Glial Progenitor Cells Exhibit a Dose-Dependent Response to Tumor-Conditioned Media (CM)

In order to examine the migratory behavior of GPC^{LacZ}, GPC^{PDGF} and XFM^{PDGF} cells, we measured the number of motile cells towards serially diluted CM gathered from the U-87, U-251 and XFM^{PDGF} tumor-derived cells. Here, we report the effective fold increase in migratory cells and the statistical significance. As shown in Fig. 3, GPC^{LacZ} cells exhibited a dosage-dependent migratory response towards U-87, U-251, and XFM^{PDGF} CM. The highest number of motile cells was measured in response to non-diluted conditioned media, 100% or CM_{100}, and was reduced when exposed to 50% diluted media, CM_{50}, and 25% diluted conditioned media, CM_{25}, from identical tumor sources. The GPC^{LacZ} cells exhibited a maximum RCF of 10 when migrating towards U-87 CM_{100} as compared to control experiments. Chemotaxis of GPC^{LacZ} cells in response to XFM^{PDGF} CM_{100} exhibited a maximum RCF of 3.9. GPC^{PDGF} cells in response to CM of U-87, U-251, and

XFM^{PDGF} exhibited RCF values of 8, 5, and 6, respectively. Similarly, XFM^{PDGF} cells in response to CM of U-87 and XFM^{PDGF} exhibited RCF values of 4 (Figs. 3a, 3c). Lastly, RCF values for all cells towards CM_{100} were reduced to 1 (i.e. level of controls) when neutralizing antibodies were used to block effects of HGF and TGF-α (data not shown).

Glial Progenitor Cells Exhibit Different Expression Levels of Cognate Receptors

We next examined GPC expression of 3 cognate receptors of key cytokines known to be highly chemoattractive to cells derived from glial tumors and present within tumor CM[4,10,27,30,70,81,83]: cMet, the receptor for HGF, Epidermal Growth Factor Receptor (EGFR), the receptor for the Epidermal Growth Factor (EGF) and TGF-α ligands, and Platelet-Derived Growth Factor Receptor beta (PDGFRβ). Western blot analysis shown in Fig. 4 illustrates that all GPC types express different levels of the 3 receptors, each benchmarked against the well-studied U-87 cell line in each experiment.[11] As seen, GPC^{LacZ}, GPC^{kRas}, and GPC^{PDGF} express cMet to approximately the same level as U-87 cells. GPC^{PDGF} and GPC^{kRas} express PDGFR at levels similar to U-87, while GPC^{LacZ} expression of PDGFR was minimal. Lastly, GPC^{PDGF} and GPC^{LacZ} expressed EGFR at levels less than U-87 and GPC^{kRas} illustrated trace amounts of EGFR.

Glial Progenitor Cells Exhibit Increased Chemotaxis in Response to Ultra Low Concentrations of Exogenous HGF, PDGF, and TGF-α

With the varying levels of GPC growth factor receptors established, the next experiments utilized transwell assays to examine the migratory responses of GPC^{LacZ}, GPC^{PDGF}, GPC^{kRas}, and U-87 cells towards different concentrations of HGF, PDGF, and TGF-α. As shown in Fig. 5, GPC^{LacZ} demonstrated the highest RCF value of 58 in response to a 10 pM HGF solution, an RCF of 12.7 in response to 1 pM PDGF and an RCF of 8.75 in response to 1 pM of TGF-α. By contrast, a concentration of 1 pM HGF induced motile GPC^{PDGF} cells with a RCF value of 8, while 100 pM TGF-α induced a 9-fold migration response in GPC^{PDGF} cells over controls. The migration of GPC^{kRas} cells was highest when exposed to a solution of 1 pM TGF-α, exhibiting an RCF value of 38, an RCF value of 10 toward 1 pM HGF, and an RCF value of 4 toward 1 pM HGF. Lastly, U-87 cells exhibited their largest RCF value of 6.64 towards 1 nM HGF.

Glial Progenitor Cell Receptor Expression is Up- or Down-Regulated when Stimulated with Exogenous Growth Factor

While the HGF and PDGF ligands demonstrated chemotactic abilities, all subsequent experiments focused particularly on the chemotaxis induced by exogenous TGF-α because it was shown to be a chemoattractant for all of the cell types studied here; its receptor, EGFR, is an extensively-studied oncogene present in diverse tumors of varying grade[43,46]; and because it has been shown to be involved in tumor cell migration.[18,55,86] In the next experiments, western blot analysis was used to detect changes in phosphorylated EGFR (pEGFR) expression between cells that were stimulated and non-stimulated with TGF-α. Detection of pEGFR was positive in non-treated (control) populations of GPC^{LacZ}, GPC^{PDGF} and GPC^{kRas} cells, as shown in Fig. 6. The intensity of each band was normalized to a value of $I = 1$ using device software as described previously. Upon stimulation with TGF-α, elevated levels of pEGFR were detected in the GPC^{LacZ} and GPC^{PDGF} cell types with average intensity values of $I = 2.63$ and $I = 5.05$, respectively. Conversely, the average intensity of pEGFR upon TGF-α stimulation in the GPC^{kRas} cell population was lower than control, at $I = 0.49$.

The μLane System Facilitates Analysis of Cell Migration within Controlled Microenvironments

Given the varying levels of EGFR expression and differences in its regulation in response to TGF-α stimulation, we next examined how specific microenvironments of TGF-α affected the chemotaxis of the genetically-altered GPC populations studied. We examined the migration of the GPC^{LacZ}, GPC^{PDGF}, GPC^{kRas}, and U-87 cell populations within our laboratory-developed microfluidic system, the μLane, in order to identify the different migratory phenotypes and distances traveled in response to known TGF-α concentration profiles. First, no cells were present at the start of microchannel experiments, facilitating visualization of cells migrating outwards from the sink reservoir and into the microchannel over time. Second, control experiments using U-87 cells incubated within a 3D matrix without exogenous growth factors verified that the μLane system maintained cell viability for up to 7 days (data not shown). In addition, as cells were seen to begin proliferating within the μLane after 40 h, cell migration experiments were limited to a 36-h period in order to exclude effects of cell division in our analysis. Last, cell distances traveled in the μLane system were measured in 200 μm increments. We determined this number to be significant because it was the average thickness of matrix-coated filters used during transwell assays, i.e. the maximum migration distance in those initial experiments.

Figure 7 illustrates the migration of GPC^{LacZ}, GPC^{PDGF}, GPC^{kRas}, and U-87 cells within μLane microenvironments generated by using 0 pM, 10 pM and 100 pM TGF-α within 3D matrix. No GPC^{LacZ} or GPC^{PDGF} cells were seen to migrate into the channel within 36 h when no additional exogenous growth factors were added within the matrix (i.e. control experiments). In contrast, the GPC^{kRas} and U-87 cells were seen to migrate within the channel in low numbers during control experiments (Figs. 7A1–7A4). When cells were exposed to gradients generated by an initial TGF-α concentration of 10 pM, all cell populations displayed enhanced migration into the channels (Figs. 7B1–7B4). In addition, each cell type exhibited a distinct migratory phenotype. GPC^{LacZ} cells migrated as single cells, GPC^{PDGF} cells exhibited group migration, while GPC^{kRas} and U-87 MG cells migrated in close association to each other resembling chains of migrating cells. Lastly, experiments recorded that GPC^{LacZ}, GPC^{kRas}, and GPC^{PDGF} appeared chemo-repulsed from the channel entrance when exposed to a microenvironment generated using 100 pM TGF-α, while the U-87 cells remained migratory (Figs. 7C1–7C4).

The concentrations and concentration gradients experienced by cells within the μLane were then determined *via* mathematical modeling, as shown Table 1. As seen, the TGF-α concentration within the first 600 μm of the μLane was between 0 pM and 0.67 pM (4.02 pg/mL of TGF-α) when 10 pM (60 pg/mL of TGF-α concentration) was used, and an order of magnitude higher, between 0 pMand 6.7 pM (40.2 pg/mL of TGF-α), when 100 pM TGF-α was used (600 pg/mL) for chemotaxis experiments. Similarly, the concentration gradient within these same regions of the channel was approximately 6.8 pg/mL per mm of channel when 10 pM was used, and 68 pg/mL per mm of channel when 100 pM was used. We note that because the distribution of concentrations along the channel length does not reach steady-state in the system until $t = 103$ h, cells were exposed to highly nonlinear and transient concentration profiles during all experiments.

Finally, the average number of cells that migrated between three regions within the channel, i.e. 0–200 μm, 200–400 μm, and 400–600 μm, was measured in response to microenvironments generated using 10 pM TGF-α as shown in Fig. 8. As seen, between 70–80% of total migratory GPC cells exhibited maximum migration between 0–200 μm in the presence of the lowest concentration of less than 0.22 pM (1.32 pg/mL of TGF-α), located at the interface between the channel entrance and the sink reservoir. GPC^{LacZ}, GPC^{PDGF}, and GPC^{kRas} cells demonstrated that the remaining 20–30% of total migratory cells were able to

migrate between 200–400 μm in the presence of a concentrations between 0.22 pM and 0.45 pM (2.7 pg/mL of TGF-α). The majority of U-87 cells, 70%, were also seen to migrate within the first 200 μm of the microchannel, while 19% of these cells were observed to migrate between 200 μm and 400 μm into the channel. U-87 was the only cell type able to migrate distances greater than 400 μm in the channel, with total of 11% of motile cells observed at this distance.

DISCUSSION

The current study utilized *in vitro* systems to examine the chemotactic migration of genetically engineered GPCs toward cytokines known to be secreted by glial tumors for enhanced tumor growth and dispersal *in vivo*.[10,48,54]

Initial experiments first verified that GPCs of different genetic backgrounds were chemoattracted to conditioned media (CM) obtained from cultures of different tumors, as well as to different growth factors present within those CM. Our results were in agreement with the wealth of data demonstrating tumor ability to recruit a diversity of cells by varying the type and concentration of factors secreted.[25,28,37,77,82] However, it was surprising to observe that all GPC types migrated preferentially towards ultra-dilute solutions (e.g. picomolar (pM) concentrations) of growth factors when the majority of studies utilize much higher concentrations to induce the chemotaxis of glioma-derived cells.[7,28,47,56,57,61,75] To examine this further, we studied the migratory responses of each genetically-altered GPC population in response to different concentrations and gradients of TGF-α.

Our study focused primarily on this EGFR binding ligand because of the well-documented role of EGFR signaling in glioma[43,44,60,84] and the lack of genetic EGFR alteration in any of the GPCs studied. Interestingly, while the upregulation of pEGFR observed reinforced the well-established positive signal transduction required for enhanced migration,[24,78] treatment of GPC^{kRas} cells with TGF-α was also seen to result in pEGFR downregulation (Fig. 6). This was unanticipated because it suggests a negative-feedback suppression mechanism that was not observed in the cell migratory response (Fig. 5). We suggest that although the cells respond to specific growth factor concentrations in a manner that significantly enhances their migration, there exists a threshold upon where the signaling affects that drive the induced response decrease. While negative feedback is seen in a plethora of systems in biochemistry, our study is the first to document such phenomena using glial-derived cells. A detailed investigation of these signaling dynamics is currently under review in our laboratory. For the continuation of the current work, we then utilized a controlled microfluidics environment to quantitatively examine the migratory response of GPCs to known concentration profiles of TGF-α.

TGF-α microenvironments generated *via* our μLane system revealed significant findings about the migratory behavior of the GPCs examined. First, despite differences in their genetic backgrounds, all GPC populations were observed to migrate readily into the microchannel when exposed to low TGF-α concentrations, but then become largely chemorepulsed by higher concentrations of the same ligand. The microchannel images illustrate classic examples of negative feedback in migration, whereby excess ligands present when receptors have become saturated and bound eliminate or reverse the biochemical effect.[2,80] This migratory behavior is consistent with the picomolar chemoattraction measured in our initial transwell assay experiments, and is previously unreported with GPCs or glioma. While *in vivo* concentration gradients within brain remain largely unknown, as a result of its highly complex cellular and extracellular matrix structure, we suggest that ultra-low concentration gradients can be expected to be experienced by cells in different anatomical regions of brain during injury and disease. A more detailed,

quantitative estimate of concentration gradients possible in the central nervous system is currently under investigation by our group, as well as several others.[3,6]

Our corroborating data implies that the stimuli which produce migratory behavior in glial tumors may differ from those that attract GPC populations towards the bulk tumor mass. Differences in the effects of such external cues remain unexamined, and carry significant consequences for how constituent and/or recruited GPC populations respond to glioma therapies.[13,85]

Second, mathematical analysis of the concentration profiles generated within the μLane illustrated that GPCs were most chemoattracted by environments of both ultra low concentration and high concentration gradient. While gradients are well-accepted as chemotactic driving forces[42,73] published studies illustrate that chemotaxis is very cell type specific: Some cell types migrate more readily at higher concentration and gradient,[39,74] while others migrate best in shallow gradients with higher concentration.[34] Moreover, all GPCs in our study were observed to migrate much shorter distances in the microchannel than their tumor cell counterparts. These results seem divert from the characteristic patterns of GPCs capable of migrating long distances in the brain.[20,35] Rather, because GPCs become stimulated by high concentration gradients at low concentration, our data implies that GPCs may become most chemoattracted during initial gliomagenesis, where small numbers of cells express low concentrations of cytokine, rather than by larger tumors seeking to increase their heterogeneity and potential nourishment.

Last, experiments using μLane systems illustrated distinct patterns of GPC migration that were surprisingly similar to what has been reported for different types of glial tumor cells *in vivo*. Cells of oligodendrogliomas and astrocytomas have been seen to typically invade normal brain parenchyma by migrating through the white matter tracts as individuals,[16,54] similar to the single cell migration exhibited by GPC^{LacZ} cells in our study. By contrast, gliomas with sarcoma characteristics have been reported to invade the brain primarily by tracking along blood vessels[36,63] such that each cell is in close contact with its motile neighbors, i.e. exhibiting the chain cell migration observed by GPC^{kRas} cells in our study. These similarities suggest that perhaps tumors of different types and grade recruit and/or transform neighboring GPCs into cells with preferred genetic backgrounds, which then regulate cell migration mechanisms that best enhance tumor dispersal and/or growth. Such novel research direction is provocative and exciting, as GPCs have remained relatively unexplored as therapeutic agents in the treatment of glioma.

CONCLUSION

The current study is among the first to examine the *in vitro* migratory responses of GPC populations with different genetic backgrounds present in the human disease. Our novel findings of uniform GPC chemoattraction at ultra-dilute ligand concentrations coupled with short migration distances underscore the need for a more comprehensive examination of glioma dispersal and growth mechanisms that incorporates tumor interactions with localized GPC populations. In addition, analysis of differences in the migratory responses of these genetically-altered cells advocate study of GPCs as potential therapeutic targets for glioma treatment.

Acknowledgments

This work was supported by the National Science Foundation (BES 0428573) and the National Institutes of Health (CAR21118255, GMR21 071702). The authors are thankful for the contributions made by Georgina Bermudez towards the total receptor western blot data and to Veronica Rotari towards the U87 cell line migration data. The

authors thank Justin Perry for illustration of the μLane system schematic. The authors also like to thank Dr. Veronica Dudu and Dr. Robert Majeska for their technical discussions and recommendations.

References

1. Alves TR, Lima FR, Kahn SA, et al. Glioblastoma cells: a heterogeneous and fatal tumor interacting with the parenchyma. Life Sci. 2011; 89:532–539. [PubMed: 21641917]
2. Amit I, Citri A, Shay T, et al. A module of negative feedback regulators defines growth factor signaling. Nat Genet. 2007; 39:503–512. [PubMed: 17322878]
3. Assanah M, Lochhead R, Ogden A, Bruce J, Goldman J, Canoll P. Glial progenitors in adult white matter are driven to form malignant gliomas by platelet-derived growth factor-expressing retroviruses. J Neurosci Off J Soc Neurosci. 2006; 26:6781–6790.
4. Badie B, Schartner J, Klaver J, Vorpahl J. In vitro modulation of microglia motility by glioma cells is mediated by hepatocyte growth factor/scatter factor. Neurosurgery. 1999; 44:1077–1082. discussion 82–3. [PubMed: 10232541]
5. Bao S, Wu Q, Sathornsumetee S, et al. Stem cell-like glioma cells promote tumor angiogenesis through vascular endothelial growth factor. Cancer Res. 2006; 66:7843–7848. [PubMed: 16912155]
6. Benedetti S, Pirola B, Pollo B, et al. Gene therapy of experimental brain tumors using neural progenitor cells. Nat Med. 2000; 6:447–450. [PubMed: 10742153]
7. Brockmann MA, Ulbricht U, Gruner K, Fillbrandt R, Westphal M, Lamszus K. Glioblastoma and cerebral microvascular endothelial cell migration in response to tumor-associated growth factors. Neurosurgery. 2003; 52:1391–1399. discussion 9. [PubMed: 12762884]
8. Chamberlain MC. MRI in patients with high-grade gliomas treated with bevacizumab and chemotherapy. Neurology. 2006; 67:2089. author reply. [PubMed: 17159134]
9. Charles NA, Holland EC, Gilbertson R, Glass R, Kettenmann H. The brain tumor microenvironment. Glia. 2011; 59:1169–1180. [PubMed: 21446047]
10. Chicoine MR, Silbergeld DL. Mitogens as motogens. J Neurooncol. 1997; 35:249–257. [PubMed: 9440023]
11. Clark MJ, Homer N, O'Connor BD, et al. U87MG decoded: the genomic sequence of a cytogenetically aberrant human cancer cell line. PLoS Genet. 2010; 6:e1000832. [PubMed: 20126413]
12. Dai C, Celestino JC, Okada Y, Louis DN, Fuller GN, Holland EC. PDGF autocrine stimulation dedifferentiates cultured astrocytes and induces oligodendrogliomas and oligoastrocytomas from neural progenitors and astrocytes in vivo. Genes Dev. 2001; 15:1913–1925. [PubMed: 11485986]
13. Dancey J, Sausville EA. Issues and progress with protein kinase inhibitors for cancer treatment. Nat Rev Drug Discov. 2003; 2:296–313. [PubMed: 12669029]
14. Dudu V, Ramcharan M, Gilchrist ML, Holland EC, Vazquez M. Liposome delivery of quantum dots to the cytosol of live cells. J Nanosci Nanotechnol. 2008; 8:2293–2300. [PubMed: 18572640]
15. Dudu V, Able R, Rotari V, Vazquez V. Role of epidermal growth factor-triggered PI3K/Akt signaling in the migration of Medulloblastoma-derived cells. Cell Mol Bioeng. 2011 In Review.
16. Duffau H, Khalil I, Gatignol P, Denvil D, Capelle L. Surgical removal of corpus callosum infiltrated by low-grade glioma: functional outcome and oncological considerations. J Neurosurg. 2004; 100:431–437. [PubMed: 15035278]
17. Duntsch C, Zhou Q, Weimar JD, Frankel B, Robertson JH, Pourmotabbed T. Up-regulation of neuropoiesis generating glial progenitors that infiltrate rat intracranial glioma. J Neuro-oncol. 2005; 71:245–255.
18. El-Obeid A, Bongcam-Rudloff E, Sorby M, Ostman A, Nister M, Westermark B. Cell scattering and Low Concentration Microenvironments 139 migration induced by autocrine transforming growth factor alpha in human glioma cells in vitro. Cancer Res. 1997; 57:5598–5604. [PubMed: 9407973]
19. Engebraaten O, Bjerkvig R, Pedersen PH, Laerum OD. Effects of EGF, bFGF, NGF and PDGF(bb) on cell proliferative, migratory and invasive capacities of human brain-tumour biopsies in vitro. Int J Cancer. 1993; 53:209–214. [PubMed: 8381111]

20. Farin A, Suzuki SO, Weiker M, Goldman JE, Bruce JN, Canoll P. Transplanted glioma cells migrate and proliferate on host brain vasculature: a dynamic analysis. Glia. 2006; 53:799–808. [PubMed: 16541395]
21. Fomchenko EI, Dougherty JD, Helmy KY, et al. Recruited cells can become transformed and overtake PDGF-induced murine gliomas in vivo during tumor progression. PLoS ONE. 2011; 6:e20605. [PubMed: 21754979]
22. Glass R, Synowitz M, Kronenberg G, et al. Glioblastoma-induced attraction of endogenous neural precursor cells is associated with improved survival. J Neurosci Off J Soc Neurosci. 2005; 25:2637–2646.
23. Goldman CK, Kim J, Wong WL, King V, Brock T, Gillespie GY. Epidermal growth factor stimulates vascular endothelial growth factor production by human malignant glioma cells: a model of glioblastoma multiforme pathophysiology. Mol Biol Cell. 1993; 4:121–133. [PubMed: 7680247]
24. Grotendorst GR, Soma Y, Takehara K, Charette M. EGF and TGF-alpha are potent chemoattractants for endothelial cells and EGF-like peptides are present at sites of tissue regeneration. J Cell Physiol. 1989; 139:617–623. [PubMed: 2786881]
25. Guo P, Hu B, Gu W, et al. Platelet-derived growth factor-B enhances glioma angiogenesis by stimulating vascular endothelial growth factor expression in tumor endothelia and by promoting pericyte recruitment. Am J Pathol. 2003; 162:1083–1093. [PubMed: 12651601]
26. Hambardzumyan D, Amankulor NM, Helmy KY, Becher OJ, Holland EC. Modeling adult gliomas using RCAS/t-va technology. Trans Oncol. 2009; 2:89–95.
27. Hata N, Shinojima N, Gumin J, et al. Platelet-derived growth factor BB mediates the tropism of human mesenchymal stem cells for malignant gliomas. Neurosurgery. 2010; 66:144–156. discussion 56–7. [PubMed: 20023545]
28. Heese O, Disko A, Zirkel D, Westphal M, Lamszus K. Neural stem cell migration toward gliomas in vitro. Neuro-oncology. 2005; 7:476–484. [PubMed: 16212812]
29. Higginbotham H, Yokota Y, Anton ES. Strategies for analyzing neuronal progenitor development and neuronal migration in the developing cerebral cortex. Cereb Cortex. 2011; 21:1465–1474. [PubMed: 21078821]
30. Hoelzinger DB, Demuth T, Berens ME. Autocrine factors that sustain glioma invasion and paracrine biology in the brain microenvironment. J Natl Cancer Inst. 2007; 99:1583–1593. [PubMed: 17971532]
31. Holland EC. Mouse models of human cancer as tools in drug development. Cancer Cell. 2004; 6:197–198. [PubMed: 15380508]
32. Holland EC, Celestino J, Dai C, Schaefer L, Sawaya RE, Fuller GN. Combined activation of Ras and Akt in neural progenitors induces glioblastoma formation in mice. Nat Genet. 2000; 25:55–57. [PubMed: 10802656]
33. Holmen SL, Williams BO. Essential role for Ras signaling in glioblastoma maintenance. Cancer Res. 2005; 65:8250–8255. [PubMed: 16166301]
34. Jeon NL, Baskararn H, Dertinger S, Whitesides GM, Water LV, Toner M. Neutrophil chemotaxis in linear and complex gradients of interleukin-8 formed in a microfabricated device. Nat Biotechnol. 2002; 20:826–830. [PubMed: 12091913]
35. Kakita A, Goldman JE. Patterns and dynamics of SVZ cell migration in the postnatal forebrain: monitoring living progenitors in slice preparations. Neuron. 1999; 23:461–472. [PubMed: 10433259]
36. Kanamori M, Vanden Berg SR, Bergers G, Berger MS, Pieper RO. Integrin beta3 overexpression suppresses tumor growth in a human model of gliomagenesis: implications for the role of beta3 overexpression in glioblastoma multiforme. Cancer Res. 2004; 64:2751–2758. [PubMed: 15087390]
37. Kleihues P, Sobin LH. World Health Organization classification of tumors. Cancer. 2000; 88:2887. [PubMed: 10870076]
38. Kong Q, Able RA Jr, Dudu V, Vazquez M. A microfluidic device to establish concentration gradients using reagent density differences. J Biomech Eng. 2010; 132:121012. [PubMed: 21142326]

39. Kong Q, Majeska RJ, Vazquez M. Migration of connective tissue-derived cells is mediated by ultra-low concentration gradient fields of EGF. Exp Cell Res. 2011; 317:1491–1502. [PubMed: 21536028]
40. Lange K, Kammerer M, Saupe F, et al. Combined lysophosphatidic acid/platelet-derived growth factor signaling triggers glioma cell migration in a tenascin-C microenvironment. Cancer Res. 2008; 68:6942–6952. [PubMed: 18757408]
41. Lassman AB, Dai C, Fuller GN, Vickers AJ, Holland EC. Overexpression of c-MYC promotes an undifferentiated phenotype in cultured astrocytes and allows elevated Ras and Akt signaling to induce gliomas from GFAP-expressing cells in mice. Neuron Glia Biol. 2004; 1:157–163. [PubMed: 17047730]
42. Lauffenburger DA, Horwitz AF. Cell migration: a physically integrated molecular process. Cell. 1996; 84:359–369. [PubMed: 8608589]
43. Liu TF, Tatter SB, Willingham MC, Yang M, Hu JJ, Frankel AE. Growth factor receptor expression varies among high-grade gliomas and normal brain: epidermal growth factor receptor has excellent properties for interstitial fusion protein therapy. Mol Cancer Ther. 2003; 2:783–787. [PubMed: 12939468]
44. Lo HW. Targeting Ras-RAF-ERK and its interactive pathways as a novel therapy for malignant gliomas. Curr Cancer Drug Targets. 2010; 10:840–848. [PubMed: 20718706]
45. Lokker NA, Sullivan CM, Hollenbach SJ, Israel MA, Giese NA. Platelet-derived growth factor (PDGF) autocrine signaling regulates survival and mitogenic pathways in glioblastoma cells: evidence that the novel PDGF-C and PDGF-D ligands may play a role in the development of brain tumors. Cancer Res. 2002; 62:3729–3735. [PubMed: 12097282]
46. Maiti AK, Ghosh K, Chatterjee U, Chakrobarti S, Chatterjee S, Basu S. Epidermal growth factor receptor and proliferating cell nuclear antigen in astrocytomas. Neurol India. 2008; 56:456–462. [PubMed: 19127042]
47. Masui K, Suzuki SO, Torisu R, Goldman JE, Canoll P, Iwaki T. Glial y in the brainstem give rise to malignant gliomas by platelet-derived growth factor stimulation. Glia. 2010; 58:1050–1065. [PubMed: 20468047]
48. Mueller MM, Werbowetski T, Del Maestro RF. Soluble factors involved in glioma invasion. Acta Neurochir. 2003; 145:999–1008. [PubMed: 14628206]
49. Nakamizo A, Marini F, Amano T, et al. Human bone marrow-derived mesenchymal stem cells in the treatment of gliomas. Cancer Res. 2005; 65:3307–3318. [PubMed: 15833864]
50. Ohashi K, Yokoyama T, Nakajima Y, Kosovsky M. Methods for implantation of BD MatrigelTM matrix into mice and tissue fixation. BD Biosciences Technical Bulletin #455. 2006
51. Onishi M, Ichikawa T, Kurozumi K, Date I. Angiogenesis and invasion in glioma. Brain Tumor Pathol. 2011; 28:13–24. [PubMed: 21221826]
52. Orsulic S. An RCAS-TVA-based approach to designer mouse models. Mamm Genome Off J Int Mamm Genome Soc. 2002; 13:543–547.
53. Park DM, Rich JN. Biology of glioma cancer stem cells. Mol Cells. 2009; 28:7–12. [PubMed: 19655094]
54. Pedersen PH, Edvardsen K, Garcia-Cabrera I, et al. Migratory patterns of lac-z transfected human glioma cells in the rat brain. Int J Cancer. 1995; 62:767–771. [PubMed: 7558428]
55. Pedersen PH, Ness GO, Engebraaten O, Bjerkvig R, Lillehaug JR, Laerum OD. Heterogeneous response to the growth factors [EGF, PDGF (bb), TGFalpha, bFGF, IL-2] on glioma spheroid growth, migration and invasion. Int J Cancer. 1994; 56:255–261. [PubMed: 8314309]
56. Pollack IF, Randall MS, Kristofik MP, Kelly RH, Selker RG, Vertosick FT Jr. Response of low passage human malignant gliomas in vitro to stimulation and selective inhibition of growth factor-mediated pathways. J Neurosurg. 1991; 75:284–293. [PubMed: 1649272]
57. Qazi H, Shi ZD, Tarbell JM. Fluid shear stress regulates the invasive potential of glioma cells via modulation of migratory activity and matrix metalloproteinase expression. PLoS ONE. 2011; 6:e20348. [PubMed: 21637818]
58. Rajasekhar VK, Viale A, Socci ND, Wiedmann M, Hu X, Holland EC. Oncogenic Ras and Akt signaling contribute to glioblastoma formation by differential recruitment of existing mRNAs to polysomes. Mol Cell. 2003; 12:889–901. [PubMed: 14580340]

59. Ren H, Yang BF, Rainov NG. Receptor tyrosine kinases as therapeutic targets in malignant glioma. Rev Recent Clin Trials. 2007; 2:87–101. [PubMed: 18473993]
60. Ronellenfitsch MW, Steinbach JP, Wick W. Epidermal growth factor receptor and mammalian target of rapamycin as therapeutic targets in malignant glioma: current clinical status and perspectives. Target Oncol. 2010; 5:183–191. [PubMed: 20853178]
61. Sampetrean O, Saga I, Nakanishi M, et al. Invasion precedes tumor mass formation in a malignant brain tumor model of genetically modified neural stem cells. Neoplasia. 2011; 13:784–791. [PubMed: 21969812]
62. Schiffer D, Annovazzi L, Caldera V, Mellai M. On the origin and growth of gliomas. Anticancer Res. 2010; 30:1977–1998. [PubMed: 20651342]
63. Schwartz MS, Morris J, Sarid J. Overexpression of oncogene products can cause tumor progression without parenchymal infiltration in the rat brain. Cancer Res. 1991; 51:3595–3601. [PubMed: 1675934]
64. Shih AH, Dai C, Hu X, Rosenblum MK, Koutcher JA, Holland EC. Dose-dependent effects of platelet-derived growth factor-B on glial tumorigenesis. Cancer Res. 2004; 64:4783–4789. [PubMed: 15256447]
65. Shih AH, Holland EC. Notch signaling enhances nestin expression in gliomas. Neoplasia. 2006; 8:1072–1082. [PubMed: 17217625]
66. Sliwa M, Markovic D, Gabrusiewicz K, et al. The invasion promoting effect of microglia on glioblastoma cells is inhibited by cyclosporin A. Brain J Neurol. 2007; 130:476–489.
67. Stieber VW, Ellis TL. The role of radiosurgery in the management of malignant brain tumors. Curr Treat Options Oncol. 2005; 6:501–508. [PubMed: 16242054]
68. Tabatabai G, Wick W, Weller M. Stem cell-mediated gene therapies for malignant gliomas: a promising targeted therapeutic approach? Discov Med. 2011; 11:529–536. [PubMed: 21712019]
69. Tchougounova E, Kastemar M, Brasater D, Holland EC, Westermark B, Uhrbom L. Loss of Arf causes tumor progression of PDGFB-induced oligodendroglioma. Oncogene. 2007; 26:6289–6296. [PubMed: 17438529]
70. Tsai JC, Goldman CK, Gillespie GY. Vascular endothelial growth factor in human glioma cell lines: induced secretion by EGF, PDGF-BB, and bFGF. J Neurosurg. 1995; 82:864–873. [PubMed: 7714613]
71. Unsicker K, Vey J, Hofmann HD, Muller TH, Wilson AJ. C6 glioma cell-conditioned medium induces neurite outgrowth and survival of rat chromaffin cells in vitro: comparison with the effects of nerve growth factor. Proc Natl Acad Sci USA. 1984; 81:2242–2246. [PubMed: 6371811]
72. Visted T, Enger PO, Lund-Johansen M, Bjerkvig R. Mechanisms of tumor cell invasion and angiogenesis in the central nervous system. Front Biosci J Virtual Libr. 2003; 8:e289–e304.
73. Wang F. The signaling mechanisms underlying cell polarity and chemotaxis. Cold Spring Harbor Perspect Biol. 2009; 1:a002980.
74. Wang SJ, Saadi W, Lin F, Minh-Canh Nguyen C, Li Jeon N. Differential effects of EGF gradient profiles on MDA-MB-231 breast cancer cell chemotaxis. Exp Cell Res. 2004; 300:180–189. [PubMed: 15383325]
75. Wells JA. Binding in the growth hormone receptor complex. Proc Natl Acad Sci USA. 1996; 93:1–6. [PubMed: 8552582]
76. Wen PY, Kesari S. Malignant gliomas in adults. N Engl J Med. 2008; 359:492–507. [PubMed: 18669428]
77. Werbowetski T, Bjerkvig R, Del Maestro RF. Evidence for a secreted chemorepellent that directs glioma cell invasion. J Neurobiol. 2004; 60:71–88. [PubMed: 15188274]
78. Wong ST, Winchell LF, McCune BK, et al. The TGF-alpha precursor expressed on the cell surface binds to the EGF receptor on adjacent cells, leading to signal transduction. Cell. 1989; 56:495–506. [PubMed: 2464440]
79. Wu A, Wei J, Kong LY, et al. Glioma cancer stem cells induce immunosuppressive macrophages/microglia. Neurooncology. 2010; 12:1113–1125.
80. Wyckoff JB, Segall JE, Condeelis JS. The collection of the motile population of cells from a living tumor. Cancer Res. 2000; 60:5401–5404. [PubMed: 11034079]

81. Xie Q, Bradley R, Kang L, et al. Hepatocyte growth factor (HGF) autocrine activation predicts sensitivity to MET inhibition in glioblastoma. Proc Natl Acad Sci USA. 2012; 109:570–575. [PubMed: 22203985]
82. Xu CP, Zhang HR, Chen FL, et al. Human malignant glioma cells expressing functional formylpeptide receptor recruit endothelial progenitor cells for neovascularization. Int Immunopharmacol. 2010; 10:1602–1607. [PubMed: 20933627]
83. Yamamoto S, Wakimoto H, Aoyagi M, Hirakawa K, Hamada H. Modulation of motility and proliferation of glioma cells by hepatocyte growth factor. Jpn J Cancer Res: Gann. 1997; 88:564–577.
84. Ye F, Gao Q, Cai MJ. Therapeutic targeting of EGFR in malignant gliomas. Expert Opin Ther Target. 2010; 14:303–316.
85. Zhang J, Yang PL, Gray NS. Targeting cancer with small molecule kinase inhibitors. Nat Rev Cancer. 2009; 9:28–39. [PubMed: 19104514]
86. Zhou R, Skalli O. TGF-alpha differentially regulates GFAP, vimentin, and nestin gene expression in U-373 MG Low Concentration Microenvironments 141 glioblastoma cells: correlation with cell shape and motility. Exp Cell Res. 2000; 254:269–278. [PubMed: 10640425]
87. Zigmond SH, Hirsch JG. Leukocyte locomotion and chemotaxis. New methods for evaluation, and demonstration of a cell-derived chemotactic factor. J Exp Med. 1973; 137:387–410. [PubMed: 4568301]
88. Ziu M, Schmidt NO, Cargioli TG, Aboody KS, Black PM, Carroll RS. Glioma-produced extracellular matrix influences brain tumor tropism of human neural stem cells. J Neuro-oncol. 2006; 79:125–133.

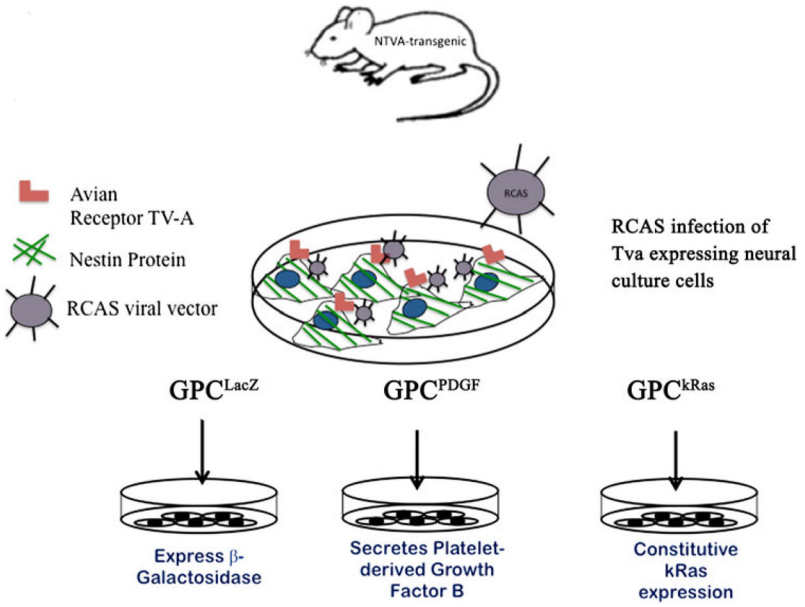

FIGURE 1.

RCAS-tv-a System used to produce GPC^{LacZ}, GPC^{PDGF}, GPC^{PDGF}, and XFM^{PDGF} cells. Ntv-a transgenic mice were created by pronuclear injection with a viral construct that contained a nestin promoter region. This infection enabled the transcription of the avian glycoprotein receptor, tv-a, in Nestin-expressing murine glial progenitor cells. Cells that expressed tv-a were then infected with various RCAS retroviruses in culture to generate GPC^{LacZ}, GPC^{PDGF}, and GPC^{kRas} cells. XFM^{PDGF} tumors were generated within mice of INK4a-$Arf^{-/-}$ background that were injected with the RCAS-PDGF-B viral vector.

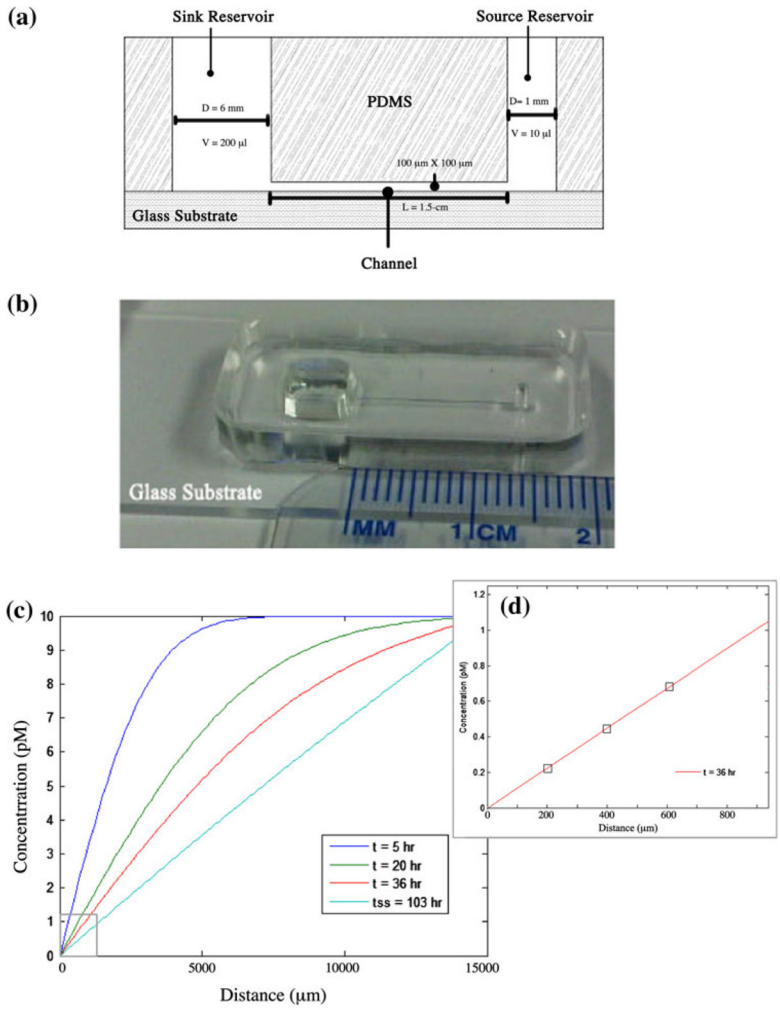

FIGURE 2.

Description of the μLane system. (a) A schematic of the μLane system comprised of a sink and source reservoir connected by a microchannel of 100 μm by 100 μm cross-section. (b) Image of a μLane system fabricated in our laboratory using glass-PDMS. (c) Mathematical simulation of the distribution of ligand concentration within the microchannel over time, *t*. (d) Inset highlights the concentration profile present within the first 1000 μm of the channel closest to the sink reservoir at the experimental time of $t = 36$ h.

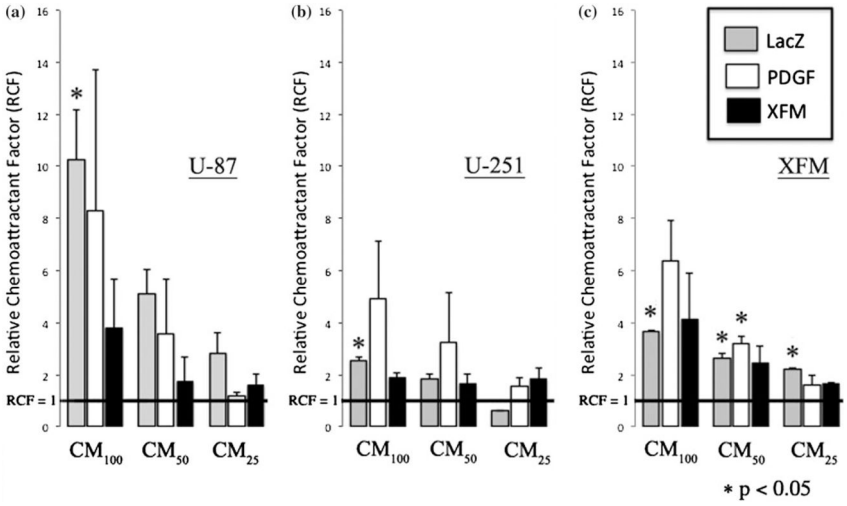

FIGURE 3.

Dose-dependent response of GPC^{LacZ}, GPC^{PDGF} and GPC^{kRas} glial progenitor cells and U-87 tumor cells to glioma conditioned media (CM). Bar graphs depict values of Relative Chemoattractant Factor (RCF), defined as the number of motile cells towards experimental conditions normalized by the number of motile cells towards control conditions (in this case non-supplemented DMEM). The normalized number of motile cells measured in response to non-diluted conditioned media, CM_{100}, 50% conditioned media, CM_{50}, and 25% conditioned media, CM_{25}, of (a) U-87, (b) U-251, and (c) XFM^{PDGF}. All experiments utilized non-supplemented DMEM as controls (i.e. RCF = 1). $p \leq 0.05$ *means significances.

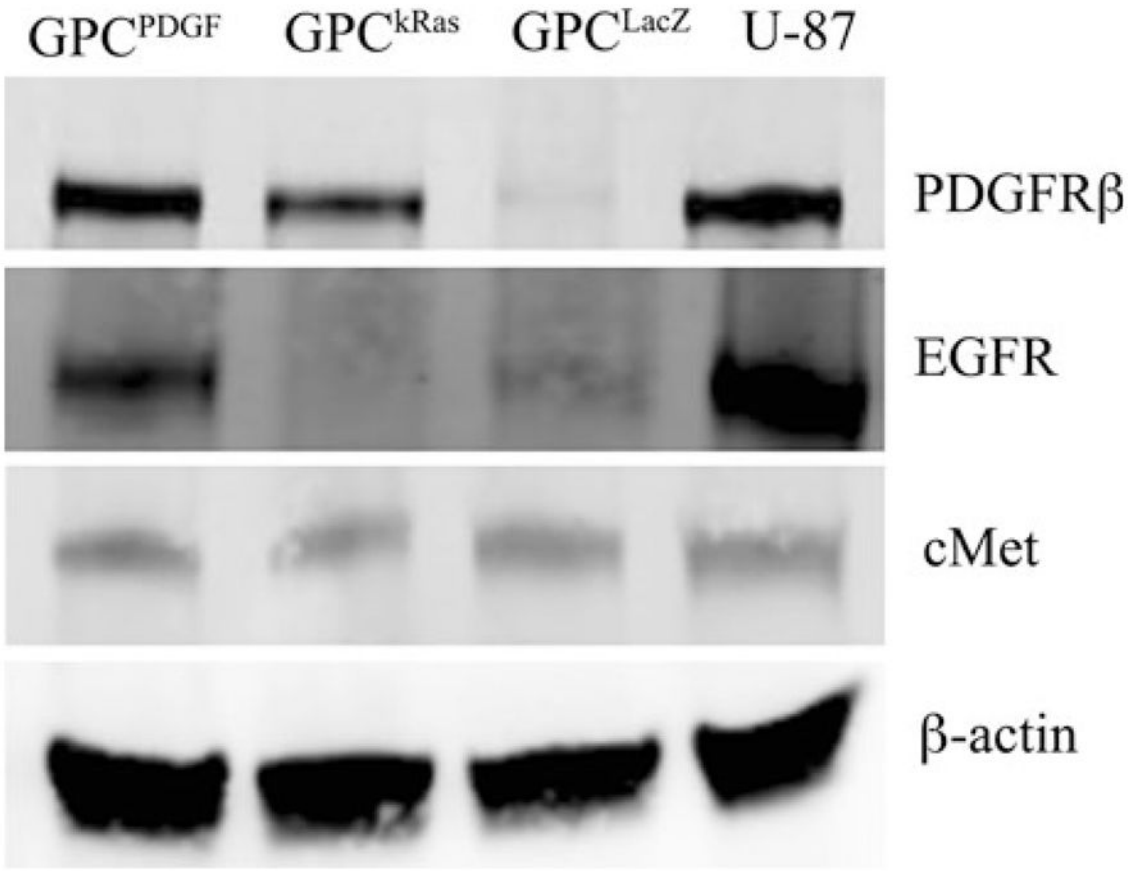

FIGURE 4.

GPC^{PDGF}, GPC^{kRas}, GPC^{LacZ}, and U-87 cell expression of total Platelet Derived Growth Factor Receptor (PDGFR), Epidermal Growth Factor Receptor (EGFR), and cMET (receptor for Hepatocyte Growth Factor, HGF) examined *via* Western blot analysis. β-actin was used as a loading control.

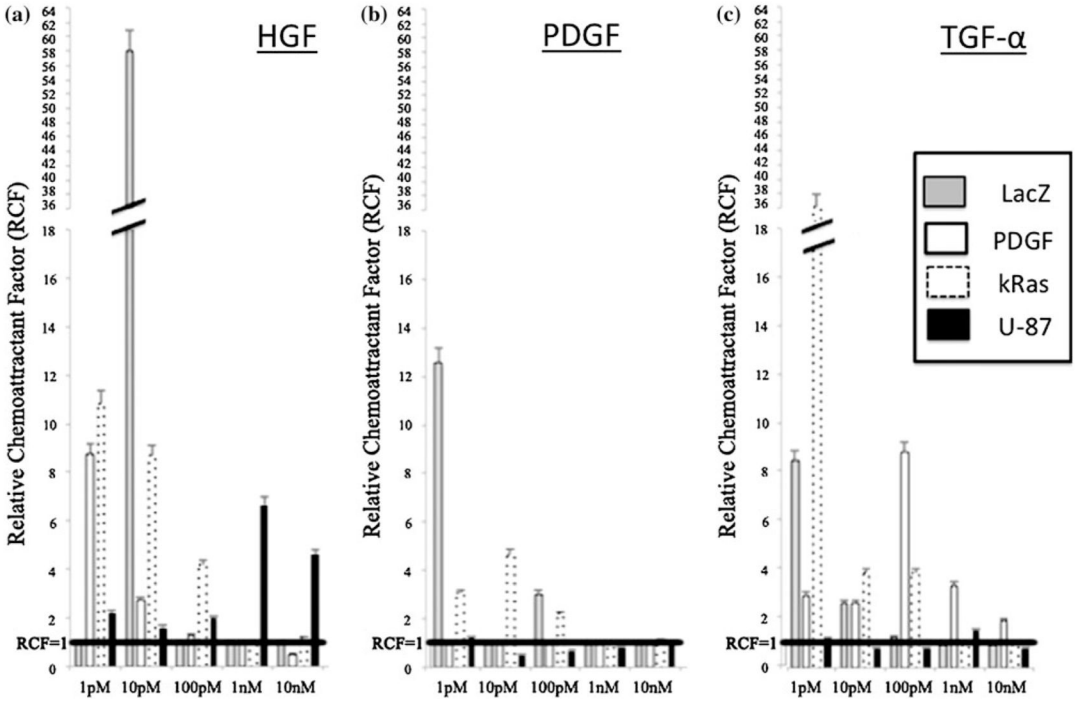

FIGURE 5.

Dose-dependent response of GPC^{LacZ}, GPC^{PDGF}, GPC^{kRas} glial progenitor cells and U-87 tumor cells to a concentration range of the (a) Hepatocyte Growth Factor (HGF), (b) Platelet-derived Growth Factor BB (PDGF) and (c) Transforming Growth Factor-α (TGF-α). Bar graphs depict values of Relative Chemoattractant Factor (RCF), defined as the number of motile cells towards experimental conditions normalized by the number of motile cells towards exogenous growth factors.

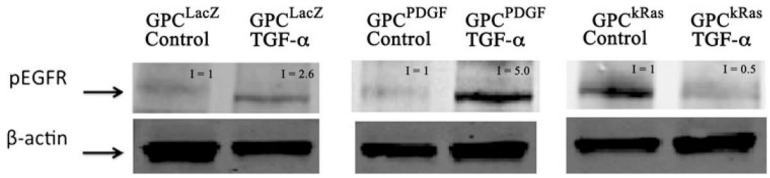

FIGURE 6.

Expression of phosphorylated Epidermal Growth Factor Receptor (pEGFR) in GPC^{LacZ}, GPC^{PDGF}, and GPC^{kRas} glial progenitor cells stimulated and unstimulated with TGF-α ligand as examined *via* Western blot analysis. The average intensity of bands, I, was divided by the intensity of bands at control conditions using device software in order to report values that reflect a fold-increase of fold-decrease of pEGFR intensity per experiment. β-actin was used as a loading control.

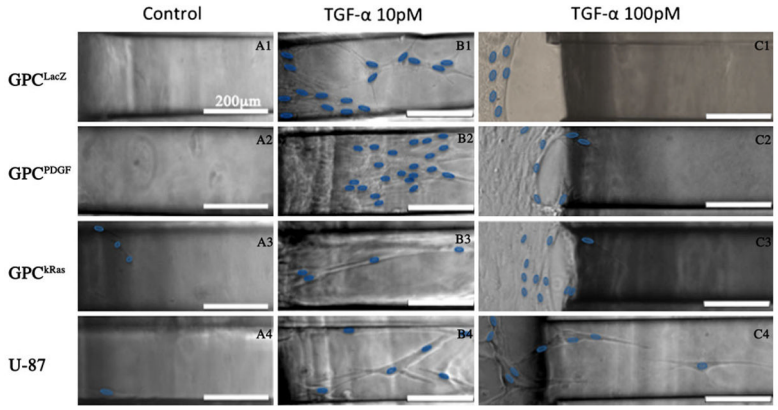

FIGURE 7.

Migration of GPC^{LacZ}, GPC^{PDGF}, GPC^{kRas}, and U-87 cells within the μLane system after 36 h in response to concentration gradients generated by using initial concentrations of (A1–A4) 0 pM (control), (B1–B4) 10 pM and (C1–C4) 100 pM of TGF-α in the sink reservoir. The left hand side of images A1–A4 and B1–B4 represent the interface between the sink reservoir and the microchannel. The nuclei of representative cells are indicated by blue ovals. Scale bars = 200 μm.

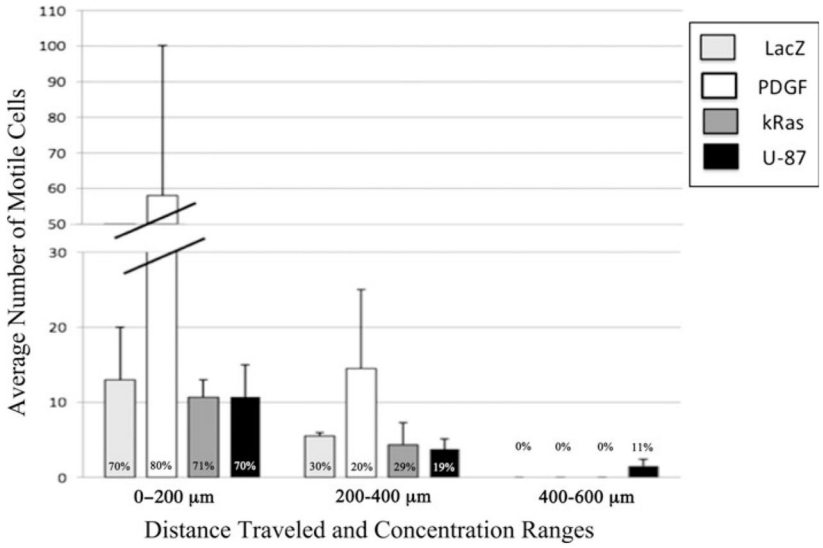

FIGURE 8.

Average numbers of migratory cells and the average maximum distances traveled within the μLane. Data was calculated using microenvironments generated 36 h after using 10 pM TGF-α in the source reservoir. The percentage of each cell type observed to migrate distances between 0–200 μm, 200–400 μm and 400–600 μm are shown.

TABLE 1

Concentrations and concentration gradients present within specified positions of the microchannel 36 h after different initial concentrations, C_0, of TGF-α were used to generate ligand concentration profiles.

	C_0 = 0 pM		C_0 = 10 pM		C_0 = 100 pM	
Distance (μm)	**C_0 (pM)**	**G (pg/mL per mm)**	**C_0 (pM)**	**G (pg/mL per mm)**	**C_0 (pM)**	**G (pg/mL per mm)**
0–200	0	0	0–0.22	6.8	0–2.2	68
200–400	0	0	0.22–0.45	6.8	2.2–4.5	68
400–600	0	0	0.45–0.67	6.8	4.5–6.7	68

Cell Mol Bioeng. Author manuscript; available in PMC 2013 November 25.